N O T I C E

THIS DOCUMENT HAS BEEN REPRODUCED FROM MICROFICHE. ALTHOUGH IT IS RECOGNIZED THAT CERTAIN PORTIONS ARE ILLEGIBLE, IT IS BEING RELEASED IN THE INTEREST OF MAKING AVAILABLE AS MUCH INFORMATION AS POSSIBLE

NAG5-15

GRAVITY AND GEOID ANOMALIES OF THE PHILIPPINE SEA: EVIDENCE ON THE DEPTH OF COMPENSATION FOR THE NEGATIVE RESIDUAL WATER DEPTH ANOMALY

By

Carl Bowin

Woods Hole Oceanographic Institution

Woods Hole, Massachusetts 02543

W.H.O.I. Contribution No. 4931

ABSTRACT

A broad regional negative free-air gravity anomaly (-10 mgal) occurs in the central part of the Philippine Sea, but geoid anomalies from GEOS-3 observations are positive. Subtraction of the geoid contribution from core-mantle boundary mass anomalies and deep mantle mass anomalies from the GEOS-3 geoid, yields a negative residual geoid anomaly consistent with the area of negative free-air gravity anomalies. Theoretical gravity-topography and geoid-topography admittance functions indicate that high density mantle at about 60 km depth can account for the magnitudes of the gravity and residual geoid anomaly and the 1 km residual water depth anomaly in the Philippine Sea. In that case, however, dense upper mantle material would be contrary to the anomalously slow surface wave velocity structure in the Philippine Sea as determined by Seekins and Teng (1977), although it could be compatible with a normal surface wave velocity structure in the west Philippine Basin as determined by Sacks and Shione (1981). Alternatively, the negative residual depth anomaly may be compensated for by excess density in the uppermost mantle, but the residual geoid and regional free-air gravity anomalies and a slow surface wave velocity structure might result from low-density warm upper mantle material lying beneath the zone of high-density uppermost mantle. From a horizontal disk approximation, the depth of the low-density warm mantle is estimated to be on the order of 200 km.

INTRODUCTION

The Philippine Sea is almost encircled by arc-trench systems: The Philippine trench, the nascent east Luzon convergent zone (Karig, 1973; Bowin, et al., 1979), the Ryukyu arc, the Nankai Trough, the Bonin arc, the Marianna arc, Yap arc, and the Palau arc. Interior to these arc systems lie four basins of increasing water depth and age (Louden, 1980) from east to west: The Marianna trough, the Parece Vela and Shikoku Basins, and the West Philippine Basin. The Marianna trough has been explained by extensional spreading behind the Marianna arc (Karig, 1971a and b, Karig et al., 1978), and the West Philippine Basin by seafloor spreading processes unrelated to plate subduction processes at an arc system (Ben-Avraham et al., 1972, Uyeda and Ben-Avraham, 1972). The depths of these basins are considerably greater than is the crust of the same age in the major oceans.

The approximately 1 km negative residual depth anomaly in the west Philippine Basin (Sclater et al., 1976) has not been adequately explained. Large free-air gravity (Watts, 1976; Watts et al., 1978) and heat flow (Sclater et al., 1976; Watanabe et al., 1977; Anderson, 1975) anomalies do not occur over the basins of the Philippine Sea. Crustal thinning by 0.5 to 2 km as suggested by seismic refraction observations (Louden, 1980) cannot fully explain the isostatic compensation for the mass deficiency of the excess water thickness compared to normal crust, nor the depression of the conductive cooling curves needed to fit the topographic data (Louden, 1980).

Surface wave velocity observations in the Philippine Sea (Seekins and Teng, 1977) indicate an anomously slow velocity structure comparable with that of warm oceanic lithosphere and upper mantle younger than 10 Ma (Forsyth, 1975). Warm material is normally associated with lower densities, whereas increased upper mantle densities of 0.01 to 0.05 g/cm^2 have been invoked (Watanabe, et

al., 1977; Yoshii, 1973) in attempts to account for the excess depths of the marginal basins. Sacks and Shiono (1981) studied group velocities of Love and Raleigh waves arriving in west Honshu, Japan and found differences between those traversing the east and west portions of the Philippine Sea. They found the velocity structure in the east to be slow, but in the west not to be slow, but similar to same aged crust elsewhere on the earth.

In this paper we examine the gravity and geoid anomalies of the Philippine Sea region in an attempt to determine the distribution and nature of possible regional mass excesses or deficiencies.

FREE-AIR GRAVITY ANOMALIES

Free-air gravity anomaly maps of the Philippine Basin have been presented by Watts (1975) and Watts et al. (1978), and show that interior to the surrounding arc systems small negative free-air anomalies predominate. A broad region of values more negative than -25 mgal occurs almost equidistant between the Luzon arc and the South Honshu Ridge which lies at the west border of the Marianna Trough. This region of low free-air anomaly values is immediately west of the Palau-Kyushu Ridge. It does not show up well in the Tasaday 7 profile presented by Sclater, et al., (1976, Fig. 3) because of the location of the ship track. It is clear, however, in the east-west profile presented in Figures 2B and 4B. In the Tasaday 7 profile, short wavelength (less than 200 km) anomalies are superimposed upon a regional low and have good correlation with topography and crustal structures. Such correlation of short wavelength features in Figure 2B is not well shown because of sparseness of gravity measurements from which the gravity data of Fig. 2B was interpolated. Broad positive anomalies occur in the West Philippine Basin adjacent to the Philippine trench and east Luzon negative anomaly belts.

If the 1 km residual depth anomaly of the West Philippine basin were

completely uncompensated, then a free-air gravity anomaly of about -96 mgal should occur. Instead, the anomalies are small indicating that isostatic equilibrium is closely achieved. Available seismic data for the West Philippine Basin indicates that the crust is about 1 km thinner than Pacific Ocean crust of the same age, but is not sufficiently thin to isostatically account for the 1 km residual depth anomaly. Thus, the causes of the negative residual depths presumably lie in the upper mantle. Assuming that most upper mantle density anomalies are thermal in nature would suggest colder than normal mantle beneath regions having negative depth anomalies. If this is so, then a positive gravitational attraction due to the excess density of the cold mantle would be expected, and might provide the compensation for the mass deficiency owing to the excess water depth. Because the topographic mass anomaly is closer than the upper mantle mass anomaly, observed free-air anomalies would be slightly negative even for perfect isostasy. This effect will be discussed quantitatively in a later section.

GEOID ANOMALIES

The geoid is that equipotential surface which coincides with mean sea-level and its extension across land areas. Prior to 1975 the geoid could only be computed from gravity observations (gravity being the vertical gradient of the earth's potential field). To be done accurately, this transformation requires gravity observations over the entire planet, a requirement that is still not met. Orbiting radar altimeters (SKYLAB, GEOS-3, SEASAT-1) now have provided direct measurements of the geoid over the world's ocean between latitudes 65° north and south. The geoid in the region of the Philippine Sea is given in Fig. 5. Marked lows occur over the Bonin and Marianna Trenches. A nearly uniform gradient crosses the Philippine Sea from south to north, and a lower gradient occurs in the area just west of the Marianna Trench low. The south

to north gradient is also evident in the geoid calculated from the perturbations of satellite orbits. These geoid solutions are generally presented as sets of spherical harmonic coefficients, such as GEM-9 (Lerch, et al., 1979).

Note that in the profile across the Philippine Sea (Fig. 2), the geoid profile is convex upward and has positive values, whereas the gravity profile is slightly concave downward and free-air gravity anomaly maps (Watts, 1976; Watts et al., 1978) indicate negative values at the center of the low. It is impossible that both these profiles can be due to the same mass anomaly. Hence they must owe their major differences to different sources. Since gravity's response to anomalous mass decreases as the square of the distance, whereas geoid anomalies simply decrease in proportion to distance, the positive regional geoid anomaly over the Philippine Sea must be due to deeper anomalies than those contributing to the regional free-air anomaly low.

Probable sources for the deeper mass anomalies that cause the positive regional geoid anomaly over the Philippine Sea have been identified in a recent decomposition of the earth's gravity field (Bowin, 1980; in prep.). That analysis followed the realization that for each spherical harmonic degree, the ratio of the gravity contribution to the geoid contribution is a greater constraint on depth and dimensions of possible source masses than is the wavelength associated with the zonal harmonics. This decomposition suggests that the mass anomalies due to topography at the core-mantle boundary and/or density anomalies in the D" layer are predominantly contained in the coefficients for the second and third harmonics, and that the harmonics 4 through 10 contain information on mass anomalies in the mantle -- largely below 300 km depth. The combined contributions from degree 4 through 10 yield a narrow belt of positive geoid anomalies coincident with most of the world's sites of plate convergence. By subtracting a degree 10 field (includes contributions

from degree 2 through 10, eg. Fig. 3A) from radar altimeter geoid observations, the contributions from mass anomalies in the deeper parts of plate convergent zones and at the core mantle boundary are largely removed. Thus, the residual geoid anomalies (eg. Fig. 4A) are restricted to those resulting from mass anomalies in the outer 600 km of the earth as would all mass anomalies contributing to degrees 11 and higher on the basis of their gravity to geoid ratio.

To evaluate better the specific regional spherical harmonic field to remove for localized studies, we plotted cumulative contribution curves for the Philippine Basin (Fig. 6). From these curves, a spherical harmonic degree 10 regional field was selected for the Philippine Basin to subtract a regional field best representing mass anomalies at the core-mantle boundary and the very broad wavelength anomaly associated with most plate convergent zones of the world (Bowin, in prep.). This spherical harmonic representation of a regional field was subtracted from GEOS-3 geoid data. A contoured map of the resulting residual geoid map is shown in Fig. 7.

The residual geoid low coincides with the area of negative free-air gravity anomalies seen in the map of Watts et al. (1978), and with the area of deep water (depths greater than 5900 m) in the West Philippine Basin (Mammerickx, 1976). The correspondence in shape of residual geoid anomaly and the regional gravity anomaly (eg. Fig. 4A and 4B) suggests that they most likely result from the same mass anomaly. This correspondence, also, provides additional support for the decomposition of the earth cited above.

ADMITTANCE FUNCTION

Variations in the thickness of the crust are not sufficient to isostatically compensate for the 1 km residual depth anomaly, in fact this mechanism would require the Moho to rise within about 1 km of the sea floor. Thus, the question arises whether the -10 mgal regional free-air anomaly and the -7m

residual geoid anomaly occurring in the center of the Philippine Basin (Figure 4A and B) result primarily from a vertical separation between the mass deficiency at the sea floor because of the greater water depth, and a mass excess which compensates for the topographic mass deficiency, or because of an uncompensated mass deficiency within the upper mantle. We, therefore, have examined the admittance function, Z, (McKenzie and Bowin, 1976; Watts, 1978; Cochran, 1979) for a structure (Fig. 8A) wherein crustal and Moho elevation perturbations are compensated by lateral mass anomalies at some depth below the Moho. Namely:

$$Z_{(k)} = \frac{g(k)}{H(k)} = 2\pi G(Pc - P_w)e^{-kd} + 2\pi G(P_m - P_c)e^{-k(d+t)} - 2\pi G(P_{dm} - P_w)e^{-k(d+tc)} \quad [1]$$

Where g(k) and H(k) are the gravity and topography response (i.e. Fourier coefficients) as a function of wave number, k. G is the gravitational constant. Pw, Pc, Pm, Pdm are densities of the water, crust, uppermost mantle, and deeper mantle, respectively. d, d+t, and d+tc are the nominal depths about which perturbations are referenced, respectively, for the seafloor topography, the base of the crust below the seafloor, and the depth of the compensating density contrast below the seafloor. Such a model assumes that the compensating mass anomalies in the mantle are concentrated at the assumed depth (the actual mass anomalies may be distributed over an extensive vertical region). The model demonstrates (Fig. 9) that the deeper the averaged depth of the compensating excess mass, the greater will be the magnitude of the observed negative gravity anomaly over the center of the residual depth anomaly feature.

From Figure 9, we can see that if the compensating mass excess is in the uppermost mantle (that is, separations of 5 to 10 km below the sea floor: i.e.

tc = 5 to 10 km) then only very small (less than -2 mgal) free-air gravity anomalies would be expected over 1 km residual depth anomalies having wavelengths greater than 1000 km. If the region of high uppermost mantle density extends over most of the east-west width of the Philippine Sea (i.e. has a larger equivalent wavelength than 4000 km), then the expected free-air gravity anomaly would be less than a milligal. If the cause of the regional -10 mgal anomaly coincides with the source of the compensation for the residual depth anomaly, then that source should lie at a depth between 25 and 100 km depending upon the appropriate wavelength (assumed to be between about 2000 and 4000 km, Fig. 9).

A geoid admittance function, Z, has been obtained by transforming the gravity admittance function (equation 1) using the filter function given by Chapman (1979). Figure 10 shows that one kilometer of residual depth anomaly would yield a residual geoid anomaly of less than one meter. If the 7 meters of the residual geoid anomaly is due to the separation between the mass deficiency of the 1 km residual depth anomaly and that of the compensating mass excess at depth, then that mass excess must lie about 60 kilometers beneath the seafloor.

DISCUSSION

A comparison of Figure 10 with Figure 9 shows that the residual geoid anomaly of -7 meters and the regional gravity anomaly of -10 mgal are only compatible with each other for a mass excess at about 60 kilometers depth that has a wavelength of about 4000 km or 2000 km half wavelength (Model A in Fig. 8). Excess mass at 60 km depth would imply colder upper mantle near that depth. Colder upper mantle material should result in faster surface wave velocity structure. However, slow surface wave velocities are found by Seekins and Teng (1977) for the Philippine Sea, and normal surface wave velocities for the

asthenosphere in the west Philippine Basin are found by Sacks and Shione (1981). For tne east Philippine Sea (Parece Vela Basin and Mariana Trough) Sacks and Shione (1981) found slow surface wave velocity structure, but this region is not tne site of the residual geoid low (Fig. 7).

The disparate group velocities determined by Seekins and Teng (1977) and by Sacks and Snione (1981) for the Philippine Sea hopefully will encourage study of other surface wave paths. Because of the large negative residual depth anomalies, and the occurrance of significant negative regional gravity and residual geoid anomalies, the Philippine Sea is an important site to investigate the structure of the upper mantle. The regional free-air gravity negative anomaly and the negative residual geoid anomaly have good spatial coincidence, but the degree of their spatial correlation with the depth anomaly remains to be clarified.

The first two possibilities presume that the negative gravity and geoid anomalies are the result of deep compensation (about 60 km) for the residual depth anomaly (Model A in Fig. 8), but attempt to explain the differing interpretations of surface wave velocity structure. One, if the surface wave velocity structure is anomalously slow, is that for reasons presently uncertain there is a paradoxical relation of younger and hotter thermal structure with negative residual depth anomalies (Louden, 1980). The second, if the surface wave velocity structure is normal, is that the compensating mass excess at depth may involve a large enough volume that its density anomaly does not significantly effect the surface wave velocity structure. The third possibility is that the depth anomaly and the gravity/geoid anomalies have independent origins. This third possibility is illustrated as Model B in Figure 8 which assumes a mass-deficiency at depth. In Figure 8B tne mass deficiency at deptn lies directly below the negative residual depth anomaly, but that need

not be the case. Both the negative depth anomaly and the compensating mass excess in the uppermost mantle may have developed in the Eocene as the lithosphere of the west Philippine basin formed. Heating of the deeper upper mantle which could cause slow surface wave velocities and the negative gravity and geoid anomalies may be a much younger phenomonon and presently be in progress.

Assuming that the source of the regional gravity and residual geoid anomalies is unrelated to the depth anomaly, what might its depth be? Because of the approximately equidimensional shape of the residual geoid anomaly pattern (Figure 8), we can estimate the depth to the mass deficiency source by assuming it occurs as a thin horizontal disc. Bowin (in prep.) presents sets of curves for gravity and geoid anomalies computed above horizontal discs with different diameters and lying at different depths. From these curves the family of various diameter and depth combinations that will produce particular gravity to geoid ratios can be easily determined. In the Philippine Sea the ratio of the regional gravity to geoid anomaly is 1.43 ($\frac{-7}{-10}$ mgals divided by $\frac{-7}{-10}$ meters; Figures 4B and 4A). Figure 11 illustrates the range of disc diameter and depth values that will produce that ratio value. From Figure 7, we infer a disc diameter of 1400 km (about 12.5^{o}), and this diameter suggests a depth to the mass deficiency of about 200 km: that is, considerably below the base of the lithosphere. Density anomalies at this depth, however, are probably not readily resolvable by surface wave velocity studies from paths limited to the dimensions of the Philippine Basin. Other modelling techniques presently under development (for example, Smith and Bowin, 1981) may provide more refined constraints on the depth and dimensions of the upper mantle anomolous mass through the use of profile and areal geoid and gravity anomaly data.

ACKNOWLEDGEMENTS

We are indebted to Donald W. Forsyth for discussion and contributing to the selection of the Philippine Sea for study. Robert Detrick helped formulate the admittance function used. We thank R. Van Wyckhouse for providing the synthetic bathymetry retrieval system. Julie Milligan, W.S. Little, and Robert Groman assisted in analysis efforts and in the development of data retrieval and processing systems utilized in this study. Review by H. Schouten and G.M. Purdy helped improve the manuscript. This study was supported by the U.S. National Aeronautics and Space Administration under Grant No. NAG 5-18.

REFERENCES

Anderson, R.N., 1975. Heat flow in the Mariana marginal basin. J. Geophys. Res., Vol. 80, p. 4043.

Ben-Avraham, A., J. Seqawa, and C. Bowin, 1972. An extinct spreading center in the Philippine Sea. Nature, Vol. 240, p. 453-455.

Bowin, C.O., R.S. Lu, C.-S. Lee, and H. Schouten, 1979. Plate convergence and accretion in Taiwan-Luzon region. AAPG Bull., Vol. 62, No. 9, p. 1645-1672.

Bowin, C.O., 1980. Why the Earth's Greatest Geoid Anomaly is so Negative. EOS, Vol. 61, No. 17, p. 209.

Bowin, C.O., in preparation. Decomposition of the Earth's Gravity Field.

Brace, K., 1977. Preliminary ocean-area geoid from Geos-3 satellite radar altimetry. Paper presented at Geos-3 meeting, NASA, New Orleans, La., Nov. 1977.

Chapman, M.E.D., 1979. Techniques for interpretation of geoid anomalies. J. Geophys. Res., Vol. 84, p. 3793-3801.

Cochran, J.R. and M. Talwani, 1977. Free-air gravity anomalies in the world's ocean and their relationship to residual elevation. Geophys. J. Roy. astr. Soc., 50, 495-552.

Cochran, J.R., 1979. An analysis of isostasy in the world's oceans, 2. Midocean ridge crests. J. Geophys. Res., Vol. 84, p. 4713-4729.

Forsyth, D.W., 1975. The early structural evolution and anisotropy of the upper mantle. Geophys. J. Roy. astr. Soc., 43, 103-162.

Karig, D.E., 1971. Origin and development of marginal basins in the western Pacific. Jour. Geophys. Res., 76, 2542-2561.

Karig, D.E., 1972. Plate convergence between the Philippines and the Ryukyo Islands. Marine Geol., Vol. 14, p. 153-168.

Karig, D.E., Roger N. Anderson and L.D. Bibee, 1978. Characteristics of Back-Arc Spreading in the Mariana Trough, J. Geophys. Res., 83, 1213-1226.

Lerch, F.J., S.M. Klosko, R.E. Laubscher, and C.A. Wagner, 1979. Gravity model improvement using GEOS 3 (GEM 9 and 10). J. Geophys. Res., Vol. 84, p. 3897-3916.

Louden, K.E., 1980. The crustal and lithospheric thicknesses of the Philippine Sea as compared to the Pacific. Earth a Planet. Sci. Letts., Vol. 50, p. 275-288.

Mammerickx, J., et al., 1976. Bathymetry of the east and southeast Asian seas. Geol. Soc. America Map Chart Series MC-17, scale 1:6,442,194.

McKenzie, D.P. and C. Bowin, 1976. The relationship between bathymetry and gravity in the Atlantic Ocean, J. Geophys. Res., 81, 1903-1915.

Sacks, I.S. and K. Shiono, 1981. Structure of the Philippine Sea Plate from Surface Waves, EOS, Vol. 62, No. 17, p. 326.

Sclater, J.G., D. Karig, L.A. Lawver and K.E. Louden, 1976. Heat flow, depth and crustal thickness of the marginal basins of the South Philippine Sea. J. Geophys. Res., Vol. 81, p. 309-318.

Seekins, L.C. and T. Teng, 1977. Lateral variations in the structure of the Philippine Sea Plate, J. Geophys. Res., 82, 317-324.

Smith, W. and C. Bowin, 1981. Mass anomaly estimation from combined inversion of gravity and geoid data (abs), EOS, Vol. 62, G 47, p. 262.

Uyeda, S. and Z. Ben-Avraham, 1972. Origin and development of the Philippine Sea. Nature Phys. Sci., Vol. 240, p. 176.

Watanabe, T., M.G. Langseth and R.N. Anderson, 1977. Heat flow in back-arc basins of the western Pacific, in: Island Arcs, Deep Sea Trenches and Back-Arc Basins, M. Talwani and W.C. Pitman, III, eds., Am. Geophys. Union, Maurice Ewing Series 1.

Watts, A.B., 1975. Gravity Field of the Northwest Pacific Ocean Basin and its Margin: Philippine Basin, Geol. Soc. Am. Map and Chart Series MC-12.

Watts, A.B., 1976. Gravity and bathymetry in the central Pacific Ocean. Jour. Geophys. Res., 81, 1533-1553.

Watts, A.B., 1978. Comment on 'On Global Gravity Anomalies and Two-Scale Mantle Convection' by Bruce D. Marsh and James G. Marsh. J. Geophys. Res., 83, 3551-3554.

Watts, A.B., C. Bowin and J. Bodine, 1978. Free-air gravity field in a Geophysical Atlas of the East and Southeast Asian Seas, The Geological Society of America, Inc., Map and Chart Series MC-25. Scale: 1:6,442,194.

Yoshii, T., 1973. Upper mantle structure beneath the North Pacific and the marginal seas. J. Phys. Earth, Vol. 21, p. 313.

FIGURE CAPTIONS

1) Philippine Sea region. Bathymetry from Mammerickx, et al. (1979) and Chase and Menard, 1969. Contour interval is 2000 uncorrected meters. Bold line indicates location of profiles shown in Figures 7-9.

2) Profiles of geoid anomaly, free-air gravity anomaly, and bathymetry across the Philippine Sea along latitude 20N. Distance scale begins at 120 E. Data obtained by interpolation from GEOS-3 radar altimeter measurements (geoid), from surface gravity measurements (free-air gravity anomaly). Bathymetric data obtained from the Synthetic Bathymetric Profiling System prepared by the Naval Ocean Research and Development Activity.

3) Profiles or regional geoid and gravity computed from GEM-9 spherical harmonic coefficients through degree 10. Same location as for Figure 2.

4) Profiles of residual geoid anomaly, residual free-air gravity anomaly, and bathymetry, obtained by subtracting regional fields (Fig. 3) from observed data (Fig. 2).

5) Geoid field measured by radar altimeter observations from GEOS-3. From Brace, 1977. Contour interval is 1 meter. Excludes contribution from earth's flattening (1/298.247).

6) Geoid cumulative degree contribution curves for selected locations in the Philippine Sea. The cumulative degree value is plotted as a function of the wavelength associated with the zonal harmonic for each individual degree. The location of the degree 10 cumulative value is labeled in each curve. Procedure follows that in Bowin (in prep.).

7) Residual geoid anomalies of the Philippine Sea region. Obtained by removing a GEM-9 spherical harmonic degree 10 field from GEOS-3 observations. Contour interval is 1 meter.

8) Two mass anomaly models that can account for the residual depth anomaly and negative gravity and geoid anomalies. RDA is the magnitude of the negative residual depth anomaly. d, t, and tc are, respectively, the nominal depths for the seafloor topography, the base of the crust below the seafloor, and the depth of the compensating density contrast below the seafloor. Pw, Pc, Pm, Pdm and densities, respectively, of the water, crust, uppermost mantle, and deeper mantle. A.) Model described by admittance function given as equation 1. See text. B.) Model in which negative residual depth anomaly is compensated by higher density uppermost mantle, and negative gravity and geoid anomalies are caused by a mass deficiency beneath the higher density uppermost mantle. (+) indicates higher density than normal, (-) lower density than normal. Thin horizontal disk approximation used in gravity/geoid ratio estimation of depth to mass deficienty.

9) Gravity-topography admittance function curves. Computed from equation 1. Curves are for different depths (tc) to compensating mass excess, labeled in kilometers. Dashed line at 10mgal/km is expected admittance to yield -10mgal amplitude for the 1 km relief to the negative residual depth anomaly in the west Philippine basin.

10) Geoid-topography admittance function curves. Transformed from the gravity-topography functions of Fig. 9 using filter function from Chapman (1979). Curves are for different depths (tc) to compensating mass excess, labeled in kilometers. Dashed line at 7 meters is expected admittance to yield -7m amplitude for the 1km relief to the negative residual depth anomaly in the west Philippine basin.

11) Depth versus diameter of horizontal disks that yield gravity to geoid ration values of 1.43 at the surface above the center of the buried disks. Circle indicates location along the g/N ratio line that corresponds with a disk diameter of 1400 km inferred from Fig. 8.

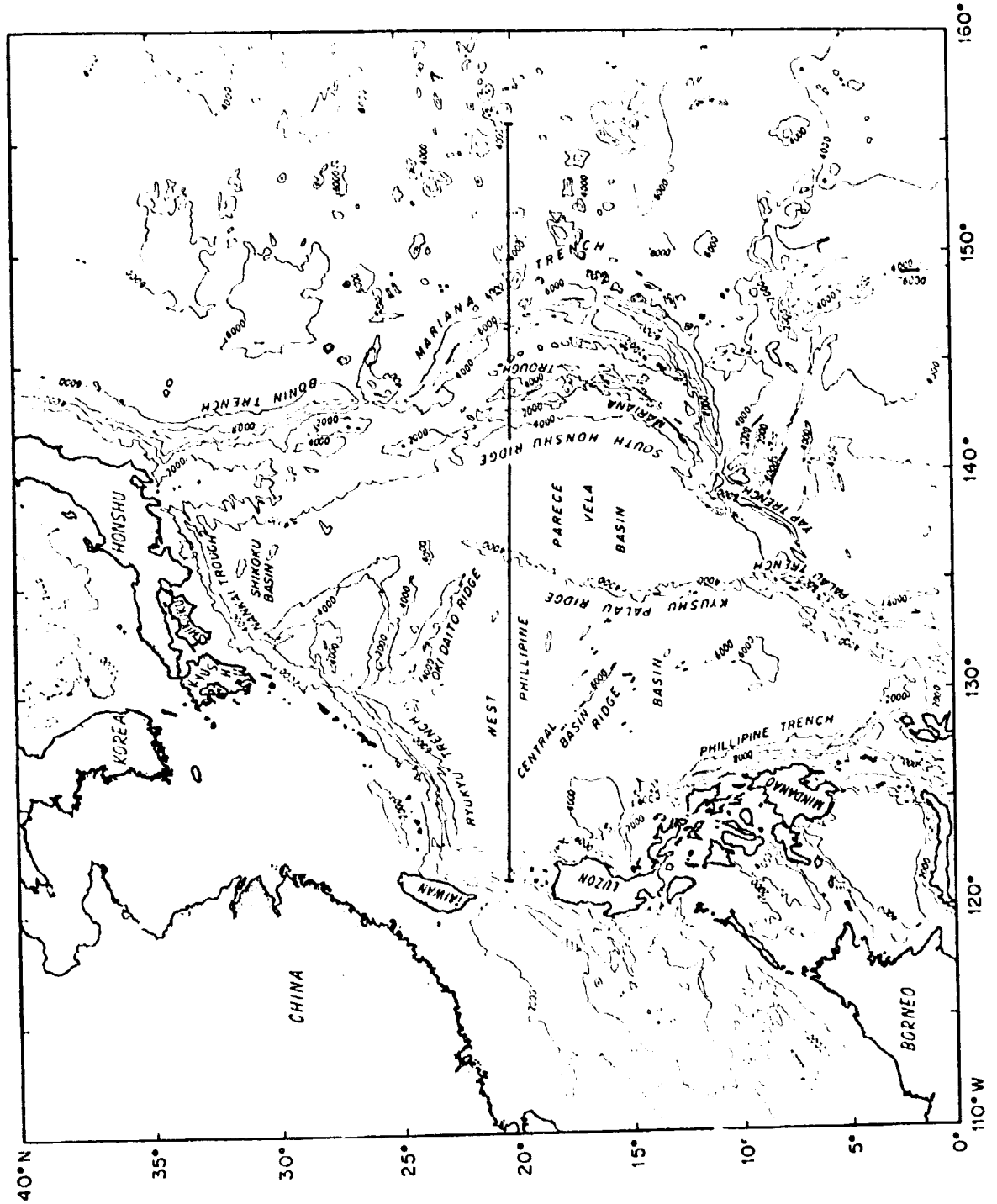

fig 1

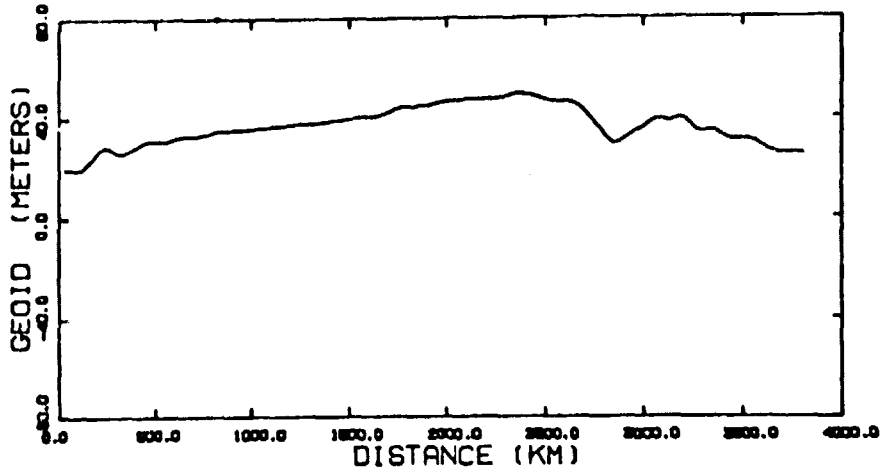

81MAY 6 11:01:16

PHILBEW1.ENN

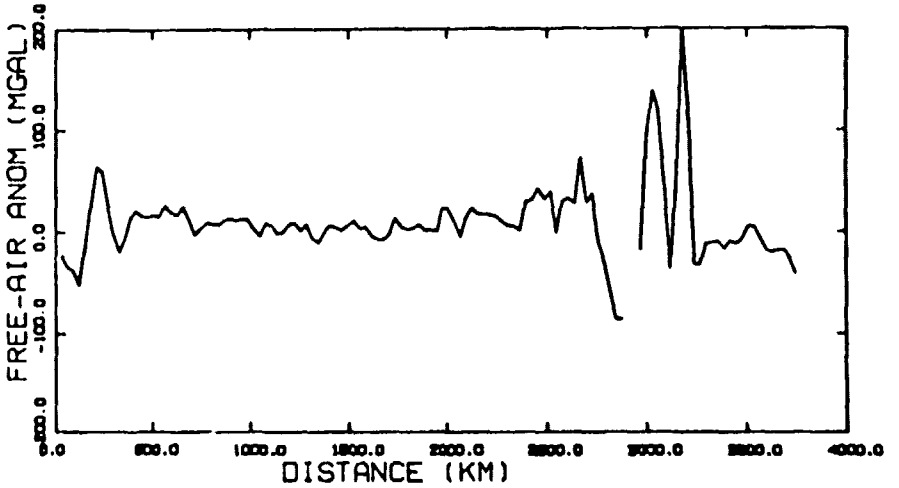

81JUN18 10:03:50

PHILBEW1.EFA

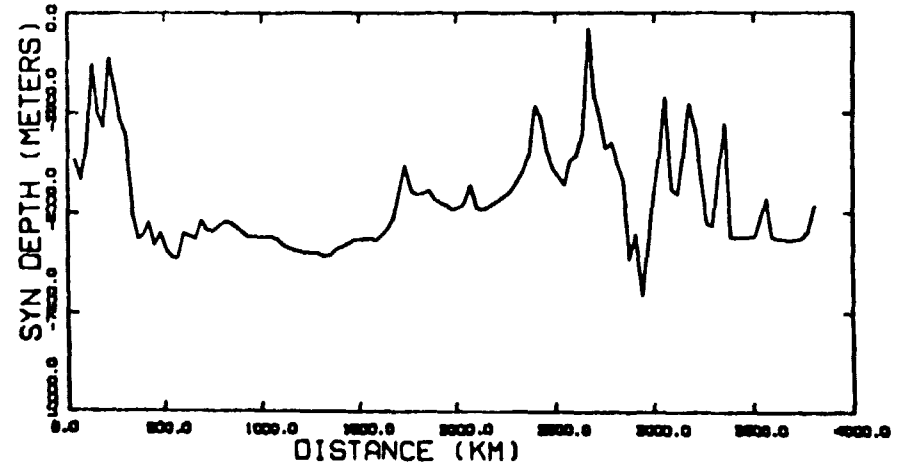

81MAY 6 11:14:27

PHILBEW1.SYB

fig 2

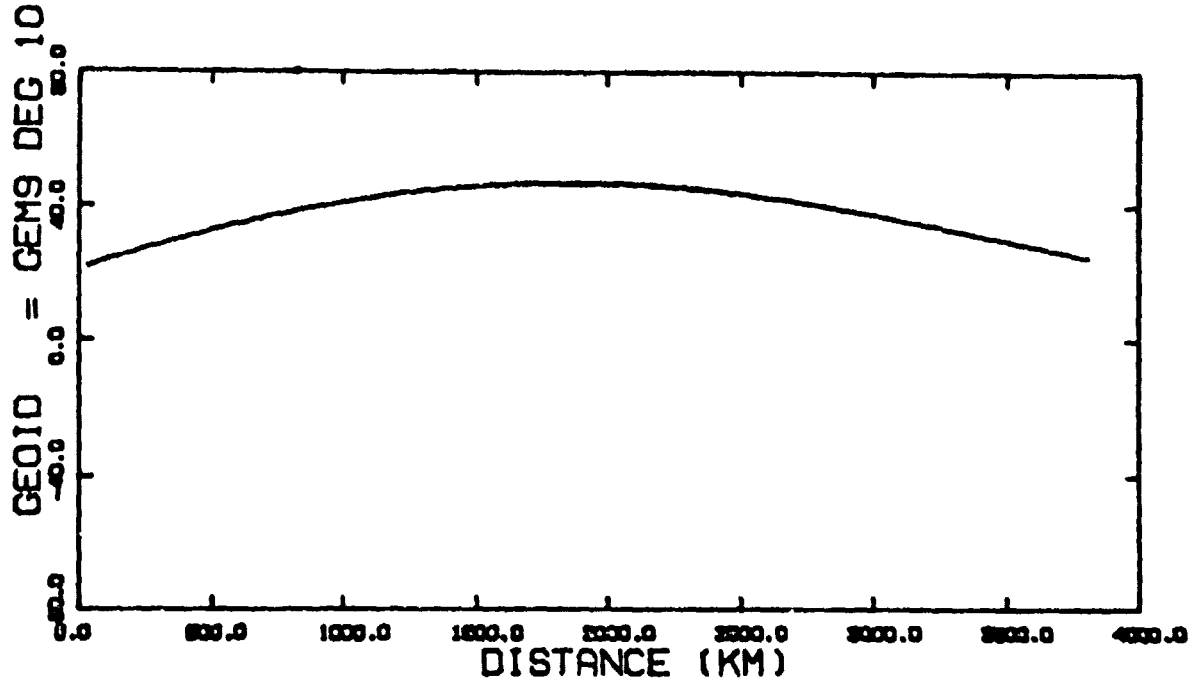

81MAY 8 11:04:48

PHILBEW1.N10

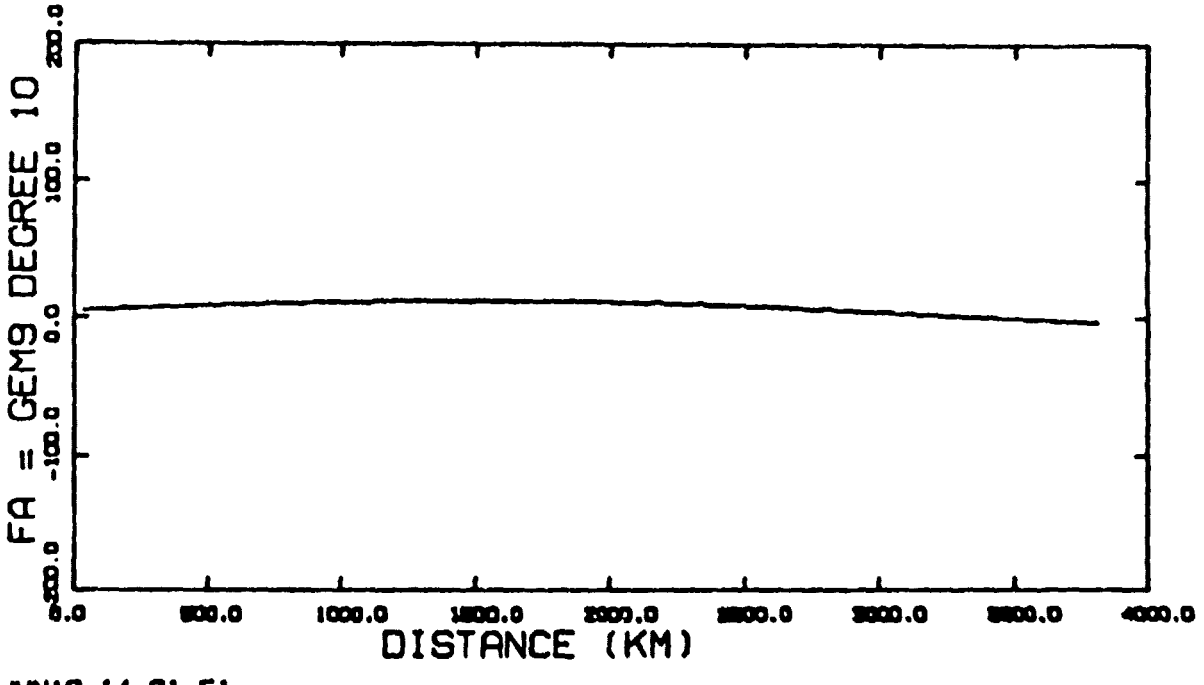

81JUN18 14:21:51

PHILBFW1.G10

fig 3

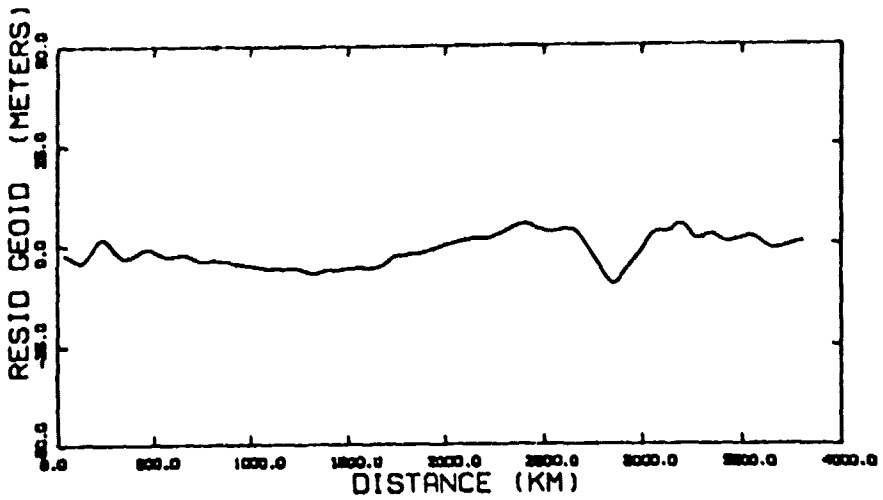

BINAY 8 11:07:11

PHILBEW1.RN1

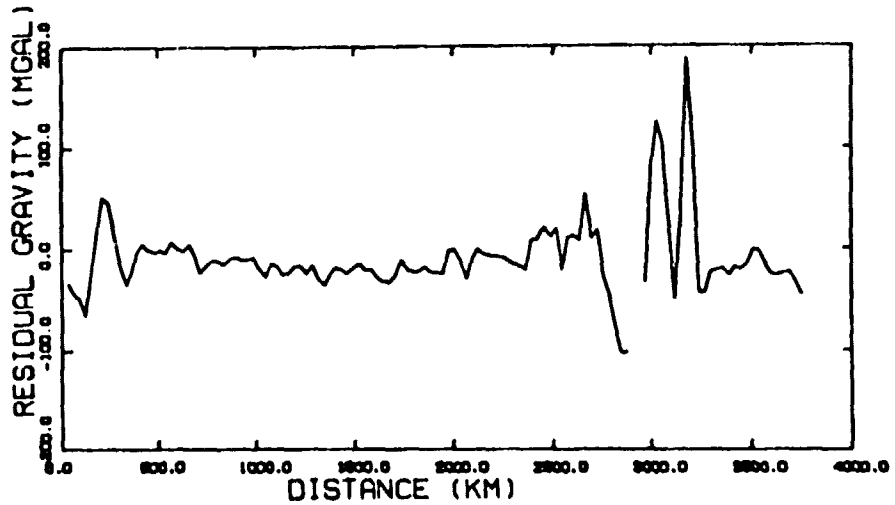

81JUN18 10:07:40

PHILBEW1.RG1

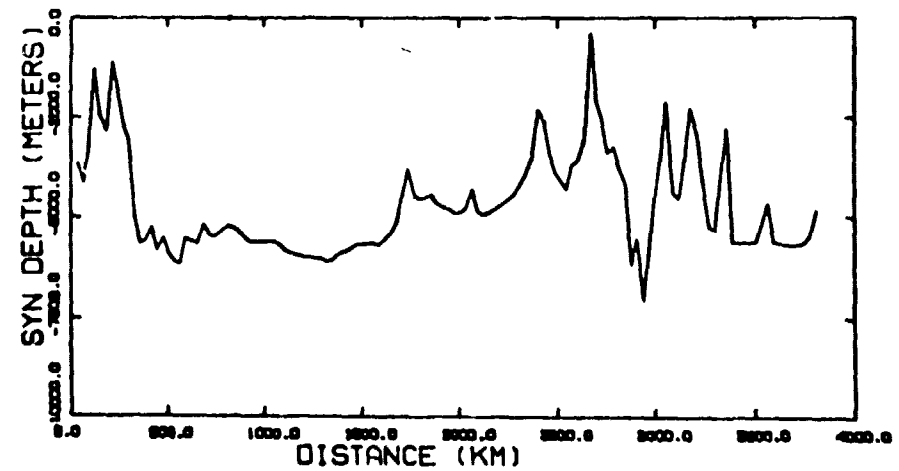

BINAY 8 11:14:27

PHILBEW1.SYB

fig 4

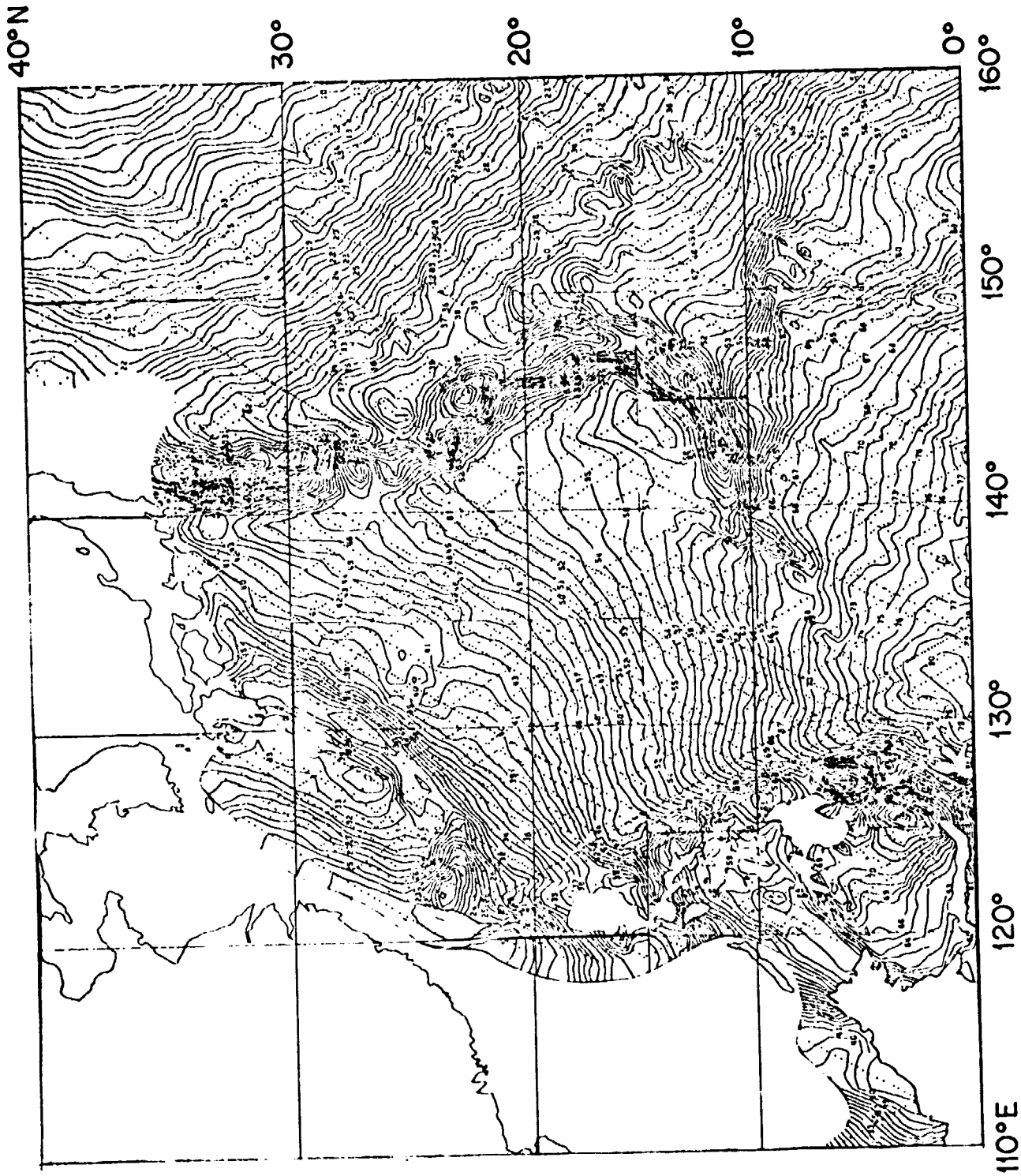

Fig 5

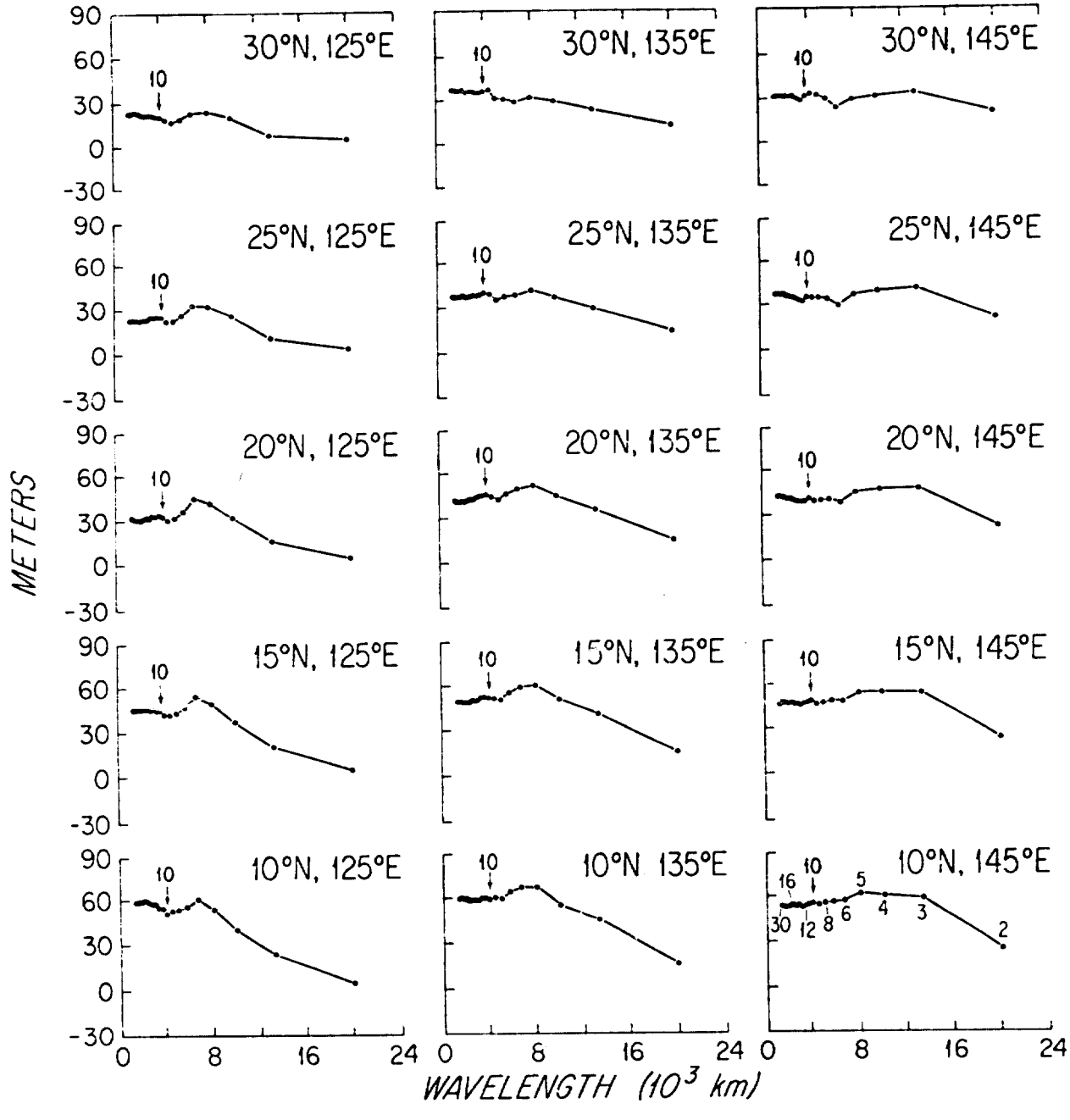
30°N, 125°E
30°N, 135°E
30°N, 145°E
25°N, 125°E
25°N, 135°E
25°N, 145°E
20°N, 125°E
20°N, 135°E
20°N, 145°E
15°N, 125°E
15°N, 135°E
15°N, 145°E
10°N, 125°E
10°N 135°E
10°N, 145°E
10
16
30
12
8
6
5
4
3
2
90
60
30
0
-30
0
8
16
24
METERS
WAVELENGTH (10³ km)

9 of 11

ORIGINAL PAGE IS
OF POOR QUALITY

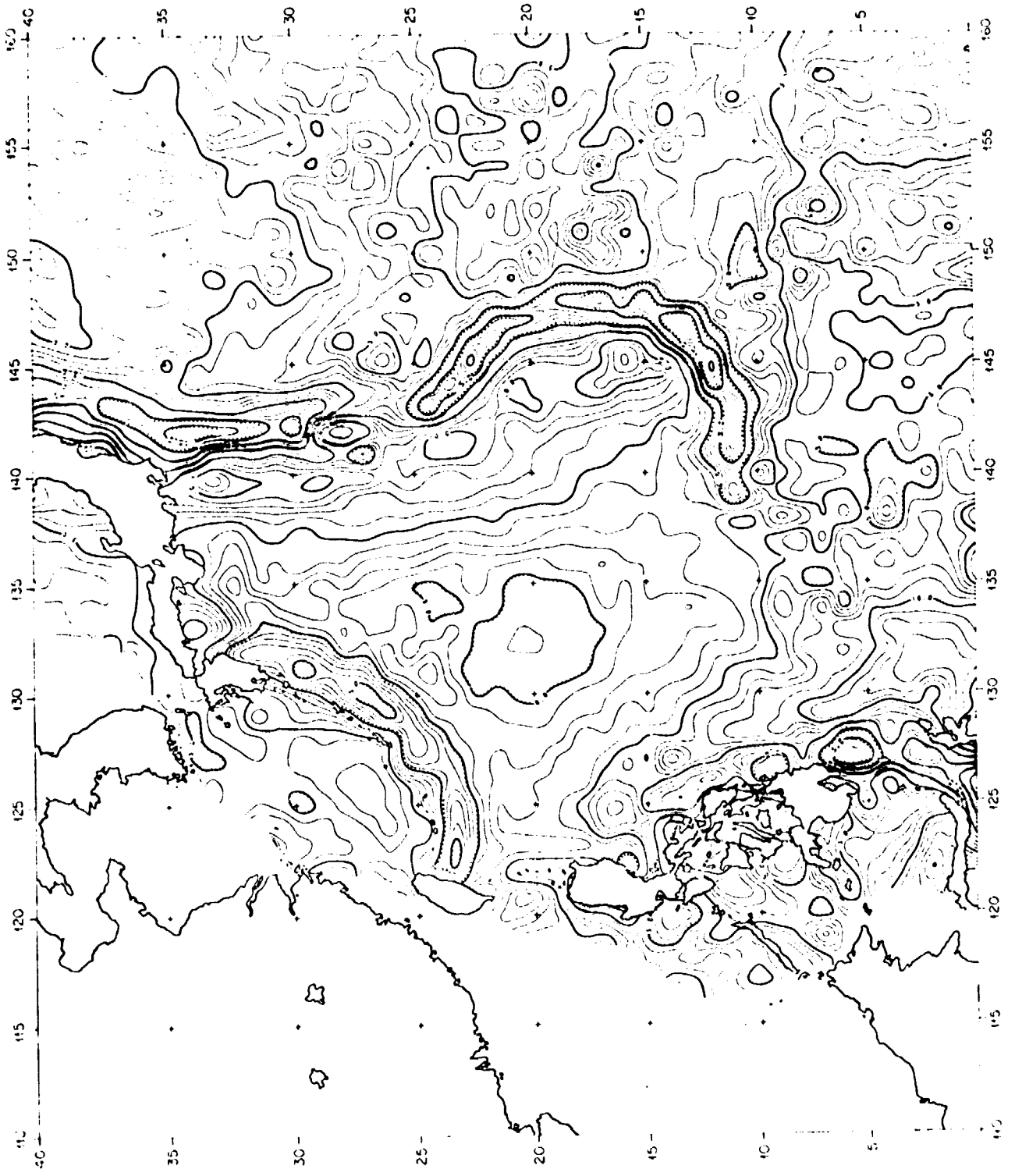

Fig 7

A

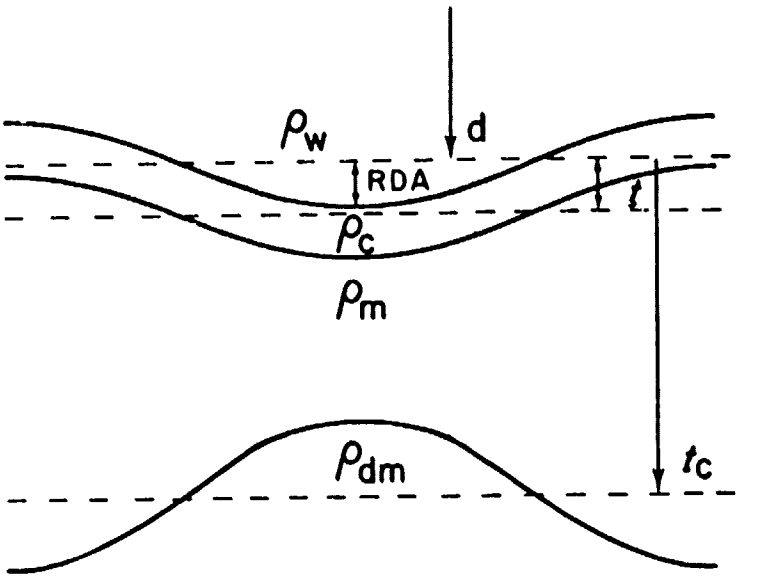

B

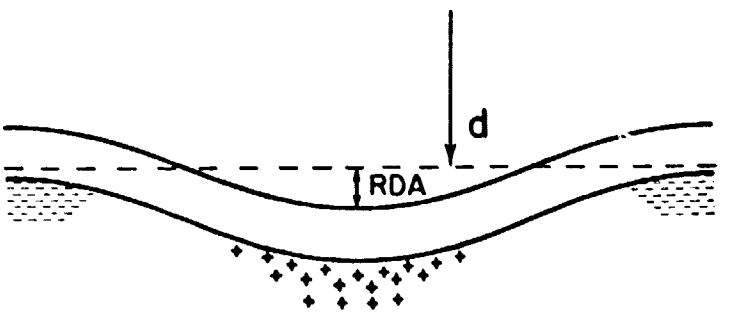

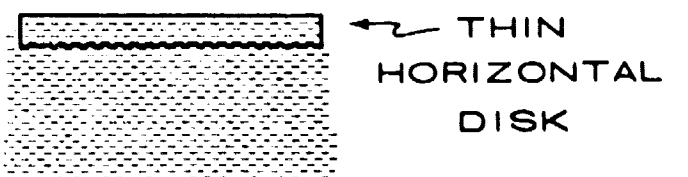

fig 8

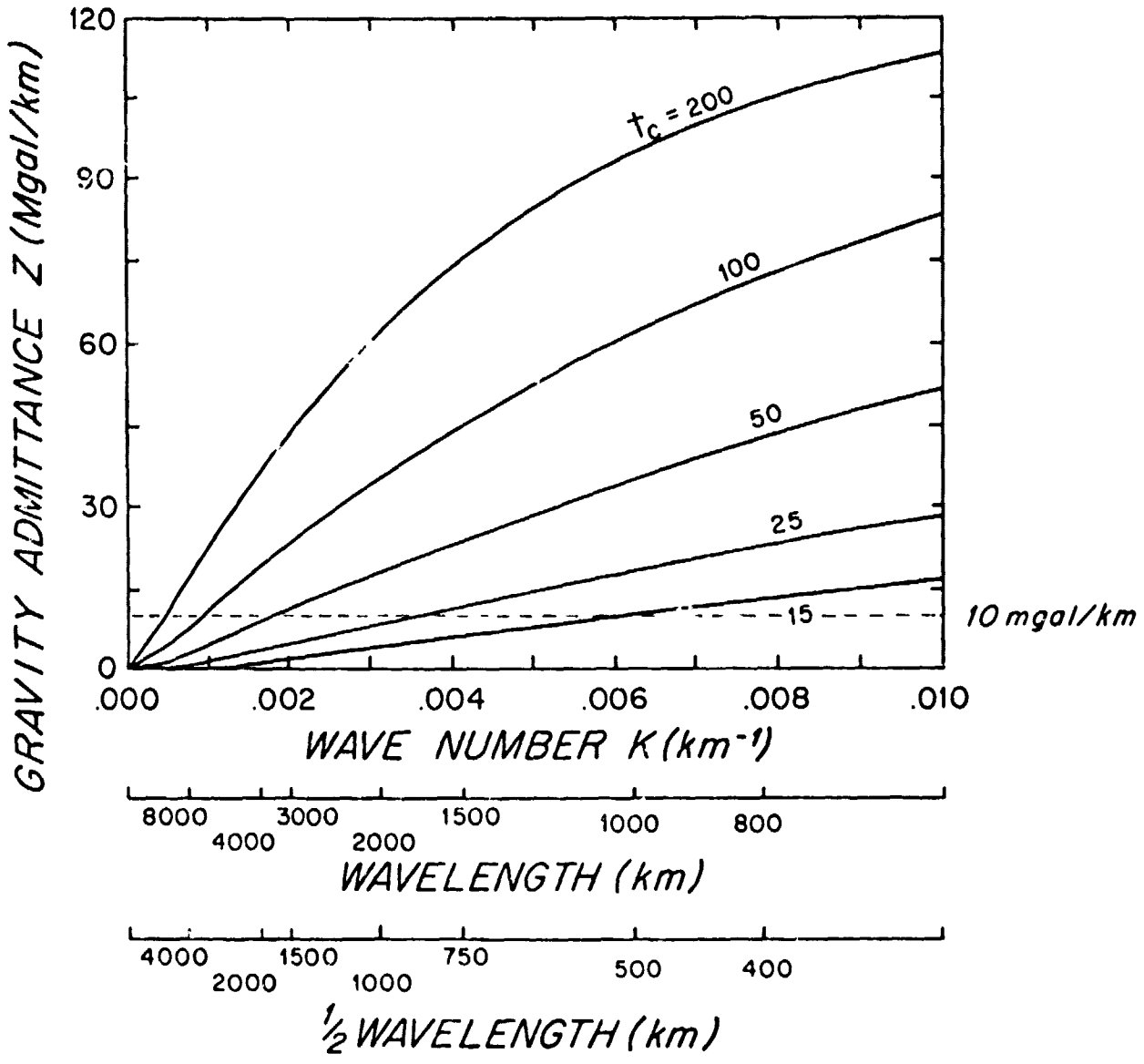
GRAVITY ADMITTANCE Z (Mgal/km)
120
90
60
30
0
t_c = 200
100
50
25
15
10 mgal/km
.000
.002
.004
.006
.008
.010
WAVE NUMBER K (km⁻¹)
8000
4000
3000
2000
1500
1000
800
WAVELENGTH (km)
4000
2000
1500
1000
750
500
400
½ WAVELENGTH (km)

Fig 9

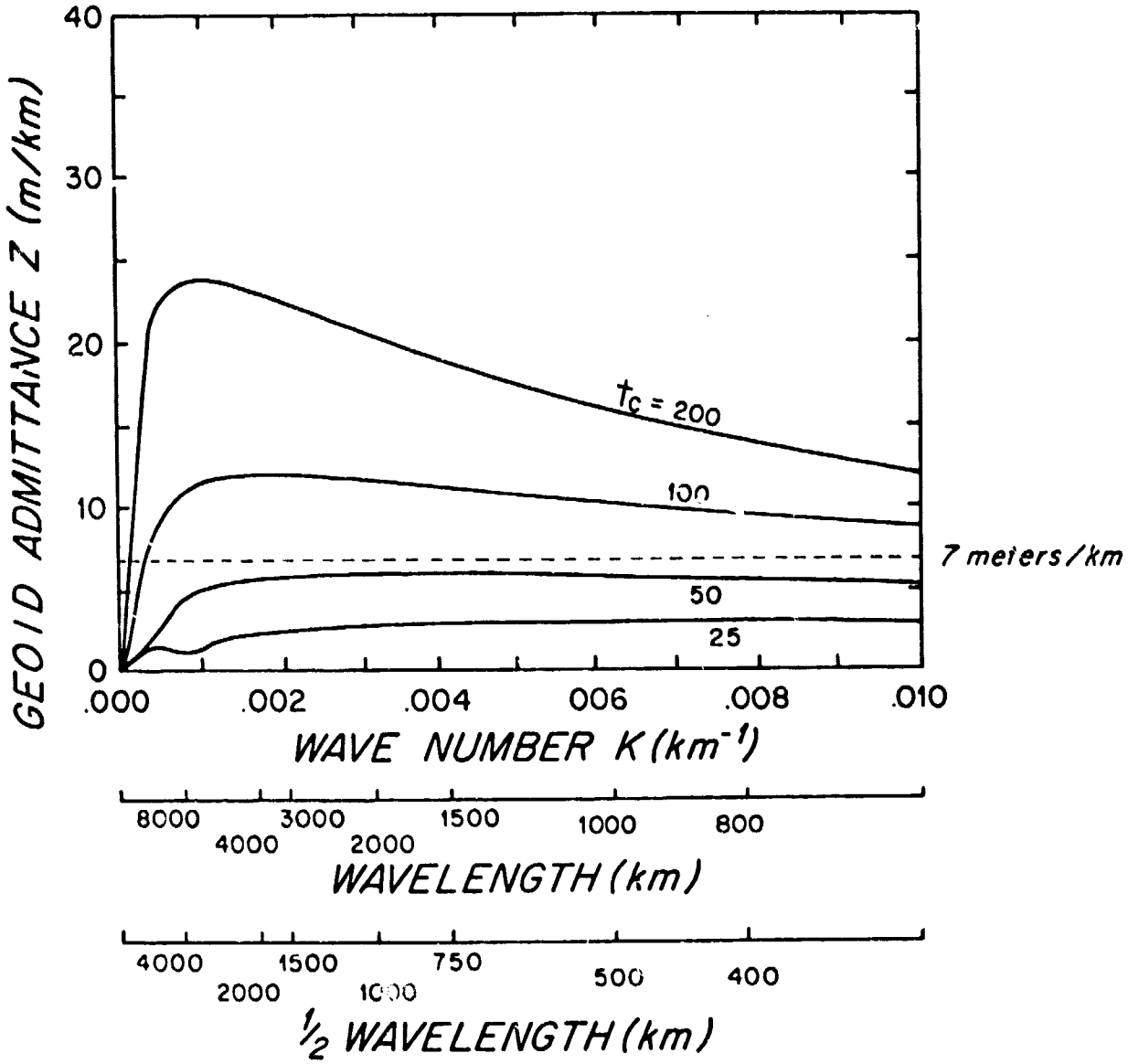
GEOID ADMITTANCE Z (m/km)
40
30
20
10
0
t_c = 200
100
7 meters/km
50
25
.000
.002
.004
006
.008
.010
WAVE NUMBER K (km^{-1})
8000
4000
3000
2000
1500
1000
800
WAVELENGTH (km)
4000
2000
1500
1000
750
500
400
½ WAVELENGTH (km)

Fig 10

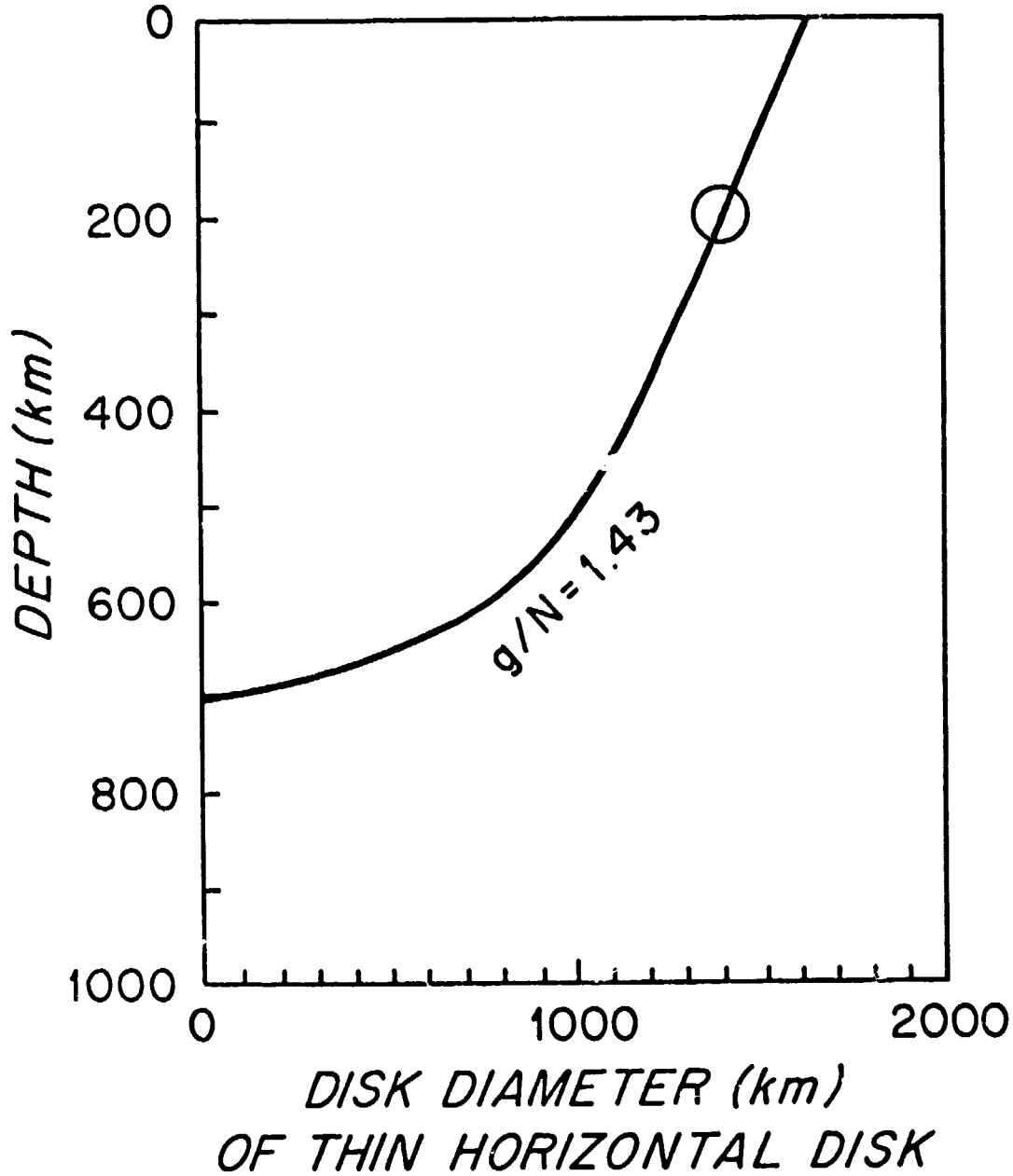
0
200
400
600
800
1000
DEPTH (km)
g/N=1.43
0
1000
2000
DISK DIAMETER (km)
OF THIN HORIZONTAL DISK

Fig 11